JOURNAL OF BACTERIOLOGY, May 2006, p. 3709–3715 Vol. 188, No. 10
0021-9193/06/$08.00+0 doi:10.1128/JB.188.10.3709–3715.2006

NOTES

D-Alanyl Ester Depletion of Teichoic Acids in *Lactobacillus plantarum* Results in a Major Modification of Lipoteichoic Acid Composition and Cell Wall Perforations at the Septum Mediated by the Acm2 Autolysin

Emmanuelle Palumbo,[1]† Marie Deghorain,[1] Pier Sandro Cocconcelli,[2] Michiel Kleerebezem,[3] Armin Geyer,[4] Thomas Hartung,[5] Siegfried Morath,[5] and Pascal Hols[1]*

Unité de Génétique, Institut des Sciences de la Vie, Université catholique de Louvain, B-1348 Louvain-La-Neuve, Belgium[1]; Istituto di Microbiologia, Università Cattolica Del Sacro Cuore, 29100 Piacenza, Italy[2]; Wageningen Centre for Food Sciences, NIZO Food Research, 6710 BA Ede, The Netherlands[3]; Institute for Organic Chemistry, University of Regensburg, 93040 Regensburg, Germany[4]; and EU Joint Research Centre, ECVAM, Ispra, Italy[5]

Received 22 November 2005/Accepted 27 February 2006

The insertional inactivation of the *dlt* operon from *Lactobacillus plantarum* NCIMB8826 had a strong impact on lipoteichoic acid (LTA) composition, resulting in a major reduction in D-alanyl ester content. Unexpectedly, mutant LTA showed high levels of glucosylation and were threefold longer than wild-type LTA. The *dlt* mutation resulted in a reduced growth rate and increased cell lysis during the exponential and stationary growth phases. Microscopy analysis revealed increased cell length, damaged dividing cells, and perforations of the envelope in the septal region. The observed defects in the separation process, cell envelope perforation, and autolysis of the *dlt* mutant could be partially attributed to the *L. plantarum* Acm2 peptidoglycan hydrolase.

Teichoic acids (TAs) are essential polymers found in gram-positive bacteria and represent up to 50% of the cell wall dry weight (17). *Lactobacillus plantarum* contains two types of TAs: lipoteichoic acids (LTA) and wall teichoic acids (WTA). The *L. plantarum* LTA are polyglycerophosphate polymers anchored in the membrane through a glycolipid. They are highly substituted with D-alanyl esters (D-Ala:phosphate [P] ratio of 0.89) and to a minor extent with glucose (Glc:P ratio of 0.11) (2). *L. plantarum* WTA are polyribitolphosphates covalently bound to the peptidoglycan via a linkage unit (22). They also carry D-Ala and Glc residues but in strain-dependent variable ratios (14).

Despite their essentiality, our understanding of the physiological role(s) of TAs is still incomplete (17). D-Alanyl substitutions strongly contribute to the function of TAs, and the study of mutants deficient in D-alanylation is of interest to expand our insight into the physiological role of these substitutents. The positively charged amino groups of D-alanyl esters partially counteract the negative charges of the backbone phosphate groups. Consequently, D-alanyl esters can modulate cell envelope properties and the function of several extracellular proteins (for a review, see reference 24). The biosynthesis of D-alanyl-LTA was extensively studied with *Lactobacillus. rhamnosus* (formerly *casei*) (10, 18, 19, 24, 25) and with *Bacillus subtilis* (27). D-Alanylation requires four proteins (DltA/Dcl, DltB, DltC/Dcp, and DltD) encoded in the *dlt* operon. In *B. subtilis*, which contains both LTA and WTA, inactivation of *dlt* genes prevents D-alanylation of both types of TAs (27). The *dlt* mutants exhibit an extended variety of phenotypes (for a review, see reference 24). For *L. plantarum*, it was recently demonstrated that the *dlt* mutant analyzed in this work displayed an enhanced anti-inflammatory capacity in a murine model of colitis (16). A large number of phenotypes can be associated with the higher-density of negative charges in the cell wall resulting from the lack of D-alanyl esters (for a review, see reference 24). As an example, TAs are thought to be involved in the control of autolysins through electrostatic interactions (12, 29). Autolysins play an important role in autolysis, cell separation, and peptidoglycan turnover, and a stimulatory effect of D-alanyl ester deprivation on autolysis has been observed in *B. subtilis*, *Staphylococcus aureus*, and *Lactococcus lactis* (23, 32, 33). In *L. lactis*, the increased autolysis of a *dltD* mutant was clearly shown to be mediated by AcmA, which is the major lactococcal autolysin involved in cell separation and autolysis in stationary phase (32).

We have recently reported the construction and the phenotypic analysis of an alanine racemase (*alr*) mutant of *L. plantarum*, which is auxotrophic for D-alanine (20, 26). Blocking D-alanine production has a pleiotropic effect, since this residue is involved in the biosynthesis of both the peptidoglycan and TAs. The phenotype of the *alr* mutant strongly suggests an activation or increased binding of autolysins. Under D-alanine starvation, the *alr* mutation resulted in loss of cell envelope integrity associated with perforations of the cell wall in the septal region, ultimately leading to cell lysis (26).

Here, we report the characterization of the *L. plantarum dlt*

* Corresponding author. Mailing address: Unité de Génétique, Institut des Sciences de la Vie, Université catholique de Louvain, 5 Place Croix du Sud, B-1348 Louvain-La-Neuve, Belgium. Phone: 32 10 47 88 96. Fax: 32 10 47 31 09. E-mail: hols@gene.ucl.ac.be.

† Present address: Laboratory of Molecular Microbiology and Biotechnology, Dipartimento di Biologia Molecolare, Università degli Studi di Siena (UNISI), Siena, Italy.

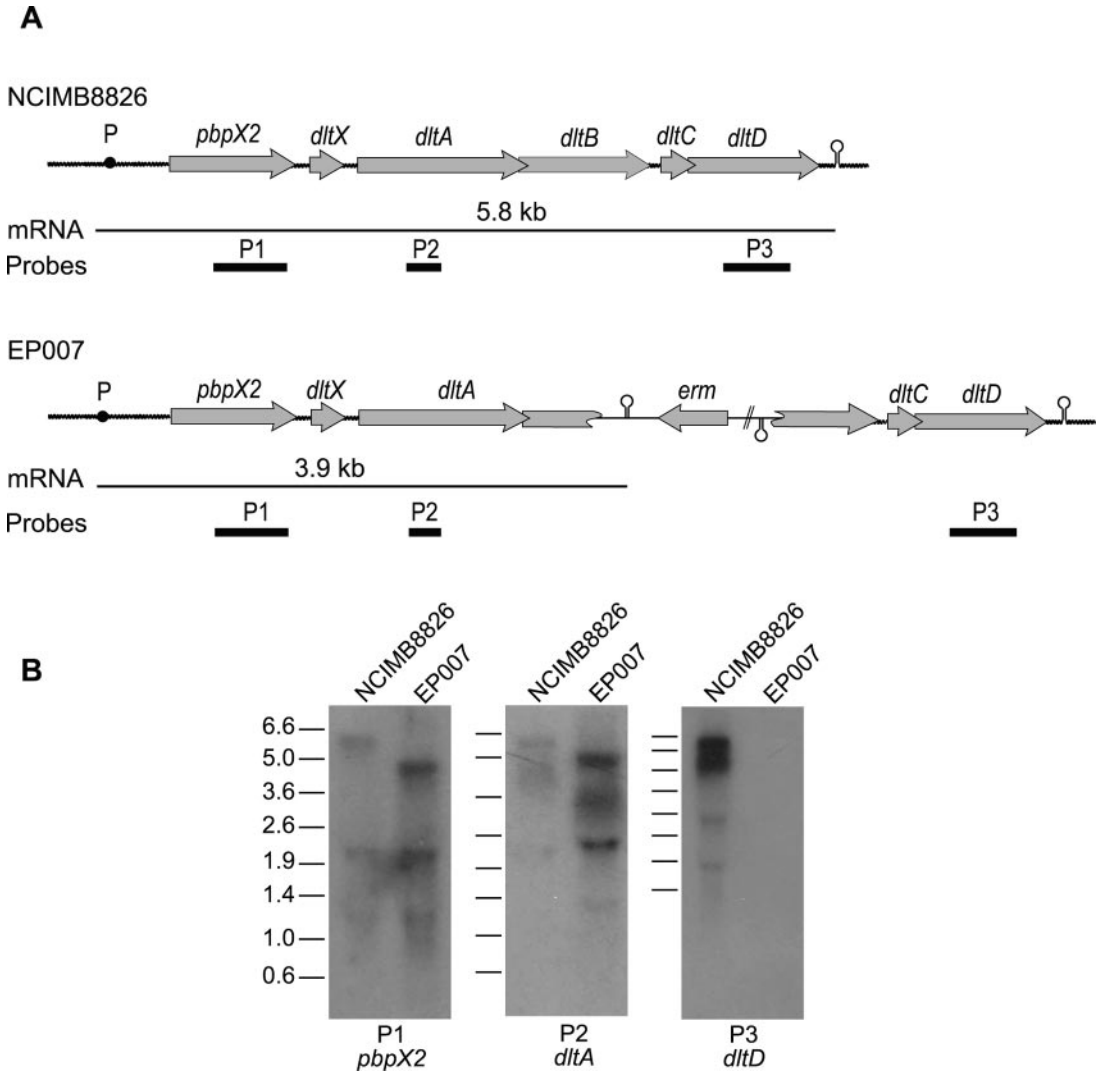

FIG. 1. Characterization and transcriptional analysis of the *dlt* operon of *L. plantarum*. (A) Genetic organization of the *dlt* operon in NCIMB8826 (wild type) and EP007 (*dlt* mutant). The probes P1, P2, and P3, used for the Northern blot experiments (see panel B), are indicated as heavy black lines. The transcripts are depicted by thin horizontal lines, and their expected sizes are indicated. The black dot represents the putative promoter (P), and the stem-loop structure represents the transcription terminator. (B) Transcriptional analysis of the *dlt* operon of the NCIMB8826 and EP007 strains by Northern blotting (13). α-^{32}P-radiolabeled PCR fragments were used as specific probes for *pbpX* (P1, primers NCIPBPX1 [5′-GGACGTCAGACAACACTTCG-3′] and NCIPBPXR2 [5′-ATAGTAATTACTCAACAGTACG-3′)], *dltA* (P2, primers LPDLT1 [5′-TCGGGATCCTCATGATAACTTGGTCAGTTACG-3′] and INVDLT3 [5′CGTATAGTGTCCCACCTAACGC-3′]), and *dltD* (P3, primers NCIDLTD1 [5′-CAAGGAACGCGGAAAGATGC-3′] and NCIDLTDR2 [5′-ACCCTTGACTCTTCAACTGG-3′]) (see panel A). DNA fragments corresponding to the reference ladder are given in kb.

mutant and the implication of D-alanylation in LTA structure, cell morphology, growth, and autolysis. Since the *dlt* mutant displays similarities in terms of lysis with the previously characterized *alr* mutant, the hypothesis that the lack of D-alanylation results in the activation or increased binding of autolysins was further verified by the analysis of a double mutant deficient in both D-alanyl esters and the autolysin Acm2.

Genetic analysis of the *dlt* locus of *L. plantarum* in the wild-type and *dlt* mutant strains. Sequence analysis of the *dlt* locus of *L. plantarum* WCFS1 (NCIMB8826 [21]) revealed the presence of two additional genes (*pbpX2* [lp_2021] and *dltX* [lp_2020]) upstream of the four *dlt* genes (*dltABCD*) previously found in other gram-positive bacteria (Fig. 1A) (1, 3, 9, 18, 25, 27, 28, 30). The presence of short intergenic sequences and the absence of putative terminators among the six genes strongly suggest that they belong to the same polycistronic unit. *pbpX2* encodes a protein showing homology to various low-molecular-weight penicillin binding proteins (PBPs) that have a D,D-carboxypeptidase activity. *dltX* encodes a putative peptide of 49 amino acids. A *dltX* homologue was systematically found upstream of *dltA* in all *dlt* clusters available from public databases. To validate cotranscription of the six genes (*pbpX2*, *dltXABCD*), total RNAs extracted from cells harvested in the exponential phase of growth were independently hybridized with three ^{32}P-labeled probes corresponding to internal fragments of *pbpX2*, *dltA*, and *dltD* (P1, P2, and P3; Fig. 1A and B).

The same transcript of the predicted size (ca. 5.8 kb) was detected with the three different probes, confirming that the six genes belong to the *dlt* operon. The additional bands below the 5.8-kb mRNA band most probably represent degradation products or nonspecific hybridization with rRNAs. A similar Northern blot analysis was performed on RNA extracted from the *L. plantarum dlt* mutant strain (EP007; *dltB*::pGIE007, erythromycin-resistant (16) (Fig. 1B). The genetic organization of the *dlt* operon in this mutant strain is depicted in Fig. 1A. A 3.9-kb transcript was detected with the probes hybridizing with *pbpX2* (P1) and *dltA* (P2), while no transcript could be detected using the *dltD* probe (P3). The 1.9-kb mRNA truncation is in agreement with the insertion of the plasmid-borne transcriptional terminator (phage λ *oop* RNA terminator) from pJDC9 (8) located downstream of the *dltB* internal fragment (Fig. 1A). Both the decreased mRNA size and the lack of *dltD* transcript detection confirmed the mutant genotype. In addition, these results indicated that strain EP007 also lacks *dltC* and *dltD* transcription but retains *pbpX2* and *dltX* transcription. Complementation of the *dlt* mutant was performed using a plasmid bearing the complete copy of the *dlt* operon (*dltXABCD*) of *L. rhamnosus* under control of its own promoter (pNZ123/*dlt*) (11). The growth defect observed in the *dlt* mutant (see below) was suppressed in the complemented strain (data not shown).

Characterization of the D-alanylation defect of LTAs. A preliminary characterization of LTA from the wild-type strain (NCIMB8826) and the *dlt* mutant (EP007) was previously reported (16). It was shown that LTA from NCIMB8826 is constituted of polyglycerophosphates (Gro-P) with D-alanyl esters as unique detectable substituents (41.7% D-Ala:Gro-P). A strong reduction in D-alanyl esters of LTA from EP007 was observed (16). During this work, a more extensive proton nuclear magnetic resonance analysis of the LTA structure from cells harvested in exponential growth phase was achieved. LTA from NCIMB8826 contain chains of 21 to 22 glycerophosphate (Gro-P) residues. Concerning the EP007 mutant, two LTA fractions were eluted from the chromatography column. The major fraction (85% of total LTA) contains threefold-longer LTA (62 to 63 Gro-P, 1.1% D-Ala:Gro-P) compared to the minor fraction (15% of total LTA, 22 to 23 Gro-P, 5.0% D-Ala:Gro-P) and to wild-type LTA. The percentage of D-alanyl esters in the EP007 mutant was strongly reduced in both LTA fractions (8- to 40-fold) compared to the wild type. Notably, the LTA from an *L. lactis dltD* mutant characterized by nuclear magnetic resonance analysis showed only a fivefold reduction in D-alanylation (5.8% D-Ala:Gro-P) compared to the wild type (28.5% D-Ala:Gro-P) (32). Interestingly, in *L. plantarum*, the longest LTA found in the major fraction is also the least D-alanylated. These results support a role of D-alanylation in polymer chain length control in LTA biosynthesis in *L. plantarum*. Strikingly, 24.2% of Gro-P residues in both fractions from the mutant are substituted with glucose, while glucose substituents were undetectable in wild-type LTA.

Growth characteristics, lysis, and cell morphology of the *dlt* mutant. The *dlt* mutant displayed different growth characteristics in comparison to the wild-type strain (as shown in Fig. 2A). The *dlt* mutant showed a lower growth rate during exponential phase, a nearly twofold-lower optical density at 600 nm (OD_{600}) at the entry of stationary phase, and a decreasing

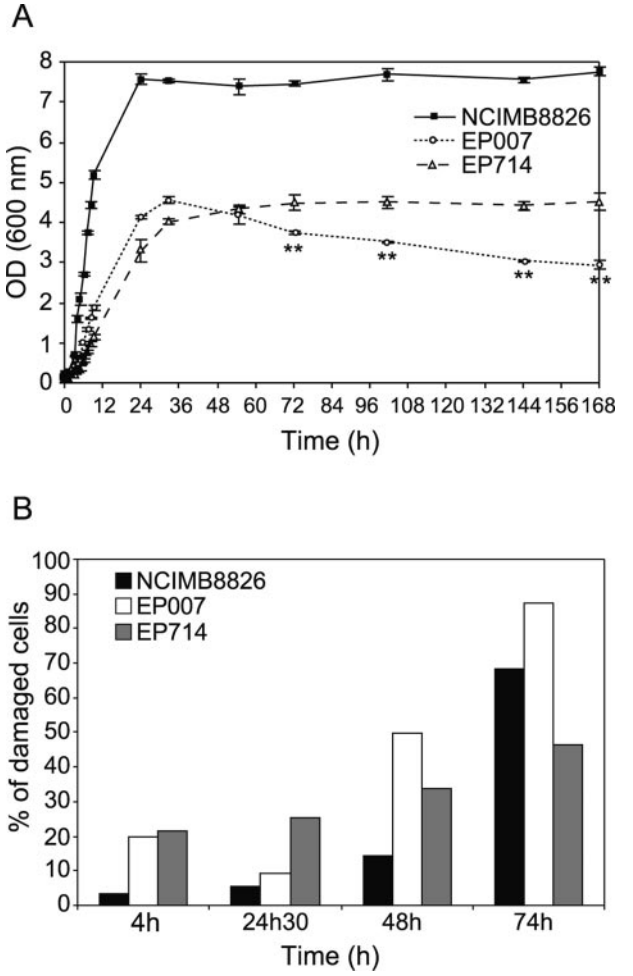

FIG. 2. Effect of *dlt* and *dlt Acm2* mutations on growth (A) and cell integrity (B). (A) Growth was measured by monitoring the OD_{600} of the NCIMB8826 strain (wild type), the EP007 mutant (*dlt*), and the EP714 mutant (*dlt acm2*) grown in MRS broth (Difco 0881, Detroit, MI) at 30°C without shaking and in the absence of antibiotics. The presence or absence of antibiotics (Em or Cm), used to maintain the integrated plasmid(s) in the chromosome, had no impact on the growth curve of the mutant strains (data not shown). Error bars represent standard deviations from the means ($n = 3$). Statistical analysis of OD_{600} values between EP007 and EP714 was performed with the Student t test. **, highly significant difference ($P < 0.01$). (B) Percentage of damaged cells was measured at different growth stages for NCIMB8826, EP007, and EP714 by epifluorescence microscopy using propidium iodide (red; labels damaged cells) and SYTO-9 (green; labels all cells). Cell samples were washed once with sterile distilled water, resuspended to about 10^{10} cells/ml, and mounted with Mowiol 4-88 medium prepared according to the manufacturer's instructions (Calbiochem-Novabiochem Corp., San Diego, Calif.). Epifluorescence microscopy was performed with a Reichert-Jung Polyvar microscope using filters B2 (fluorescein isothiocyanate, 901124) and G2 (901220). The percentage of damaged cells labeled with propidium iodide was calculated with respect to the total number of cells labeled with SYTO-9. Enumeration was done for a minimum of 300 cells for each strain. Measurements were performed in the exponential growth phase (4h), at the entry of stationary phase (24h30), and in stationary phase (48h and 74h).

OD_{600} during stationary phase, suggesting a lytic process. During stationary phase (between 24 and 72 h), the number of CFU/ml for the *dlt* mutant decreased dramatically (60%), while it remained almost unchanged for the parent strain (data

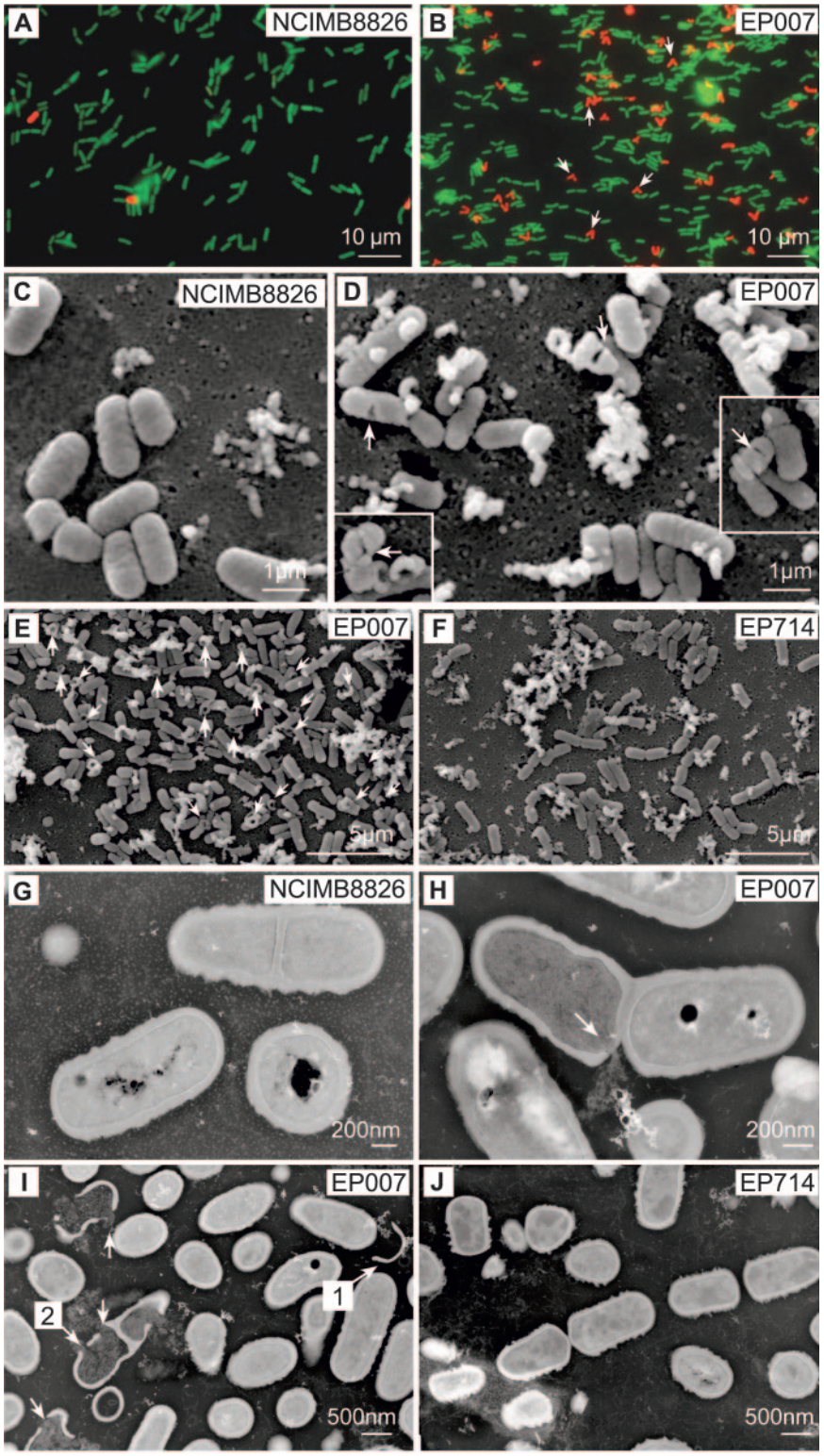

FIG. 3. Epifluorescence, scanning electron, and transmission electron micrographs of cells from NCIMB8826 (wild type; A, C, and G), EP007 (*dlt*; B, D, F, H, and I), or EP714 (*dlt acm2*; F and J). (A and B) Cells for epifluorescence microscopy were collected in exponential growth phase. Growth conditions and cell preparation were as described in the Fig. 2 legend. The arrows indicate particular V-shaped dividing cells (B). (C to F) Scanning electron microscopy was performed with cells collected in exponential growth (C and D) and in late stationary growth phase (E and F). The arrows show perforations of EP007 cells (D) that are absent in wild-type cells (C). (G to J) Transmission electron microscopy was performed with cells collected in stationary growth phase. The arrow in panel H shows a perforation located at the septum of an EP007 cell. In panel I, arrow no. 1 shows a fragment of an empty envelope and arrow no. 2 indicates a perforation at the putative next division site. The perforations visible in EP007 cells (H, I) disappear in EP714 (J).

not shown). In order to confirm this lytic process, the integrity of the membrane in the cell population was investigated by previously described fluorescence labeling with a mixture of SYTO-9 (5 μM) and propidium iodide (30 μM), which differentially labels all bacteria and injured bacteria with damaged membranes, respectively (6) (Fig. 2B and 3A and B). The percentage of injured cells (labeled in red in Fig. 3) in the *dlt* mutant was higher than in the wild type at every growth stage (Fig. 2B). The twofold decrease in injured cells observed for the *dlt* mutant at the entry of stationary phase (24 h 30 min) is probably due to a higher number of disrupted cells that are too severely damaged to be labeled at all.

Epifluorescence and electron microscopy revealed that the *dlt* disruption had an impact on cell morphology. During the exponential growth phase, EP007 cells displayed an increased length in comparison to the wild type (data not shown). A similar observation has previously been reported for the *dltD* mutant of *L. rhamnosus* (11). Epifluorescence microscopy observations revealed that a majority of damaged cells of the mutant (labeled in red) showed a V shape during exponential phase (Fig. 3B), suggesting that a lethal event occurs during the division process. Scanning and transmission electron microscopy (SEM and TEM), performed as previously reported (26), clearly showed perforations of cell envelopes (Fig. 3D, H, and I), the release of cytoplasmic material from perforated cells, empty cells, and cell envelope fragments (Fig. 3E and I). The cell perforations became more numerous in stationary phase (data not shown), corroborating the above observations on cell lysis. When the cell damage is limited to a hole (50 cells examined), the perforation is localized in the septal region (see Fig. 3H for an example); also, in some cells, additional perforations were observed at the position of the next division site (see Fig. 3I for an example).

Inactivation of the gene encoding the autolysin Acm2. It was recently shown that lysis of a *dltD* mutant of *L. lactis* clearly involved the major autolysin AcmA, which plays a role in cell separation and autolysis in stationary phase (32). Acm2 from *L. plantarum* WCFS1 (21) displayed the highest level of identity (34%) with the lactococcal AcmA protein. In addition, Acm2 contains a C-terminal domain with five repeats and an N-terminal region rich in Ala, Ser, and Thr. These two regions might be involved in cell wall binding, as previously reported for other peptidoglycan hydrolases from *L. lactis* (4, 31).

To confirm functional orthology between *L. plantarum* Acm2 and *L. lactis* AcmA, the *acm2* gene was expressed in the *acmA* mutant of *L. lactis* (5). Heterologous expression of *acm2* in this background resulted in complete suppression of the cell separation defect in the *L. lactis* mutant (data not shown), confirming the role of Acm2 as a peptidoglycan hydrolase involved in cell separation.

In order to investigate the functional role of Acm2 as a peptidoglycan hydrolase, the *acm2* gene was disrupted by a single crossover in the wild-type strain (20). A 622-bp fragment of *acm2* was PCR amplified (primers NCNAM1F1 [5′-GATCTGCAGTGAGCTGCGACTAAGGGAAACAG-3′] [PstI] and NCNAM1R2 [5′-TGCGGTACCTGACTAGTCATTGCCCGCG-3′] [KpnI]) and cloned between PstI and KpnI of the suicide plasmid pGIM008 (pACYC184 derivative containing the pC194 chloramphenicol resistance gene; M. Deghorain, unpublished), yielding pGIE014. Chromosomal integration of pGIE014 results in a 3′-end-deleted *acm2* copy encoding the putative N-terminal cell wall binding domain and a second 5′-truncated *acm2* copy, which is preceded by stop codons in the three frames to avoid any translation. Correct integration of pGIE014 at the *acm2* locus was confirmed by PCR, and the resulting mutant was designated EP114 (*acm2*::pGIE014, Cm^r).

The major characteristic of the *acm2* mutant was the appearance of chains of incompletely separated cells (Fig. 4). During the exponential phase (4 h) and the stationary phase (48 h), 30% and 60% of EP114 cells are associated in chains (3 to 13 cells), respectively (Fig. 4C), while more than 95% of the wild-type cells at any growth phase are isolated or associated in pairs (Fig. 4C). Analysis of EP114 cells by SEM and TEM showed a cell length similar to that of the wild type and a capacity to form a complete septum (data not shown).

Contribution of Acm2 to *dlt* mutant phenotype. In order to investigate the contribution of Acm2 to the lytic phenotype of the *dlt* mutant, a *dlt acm2* double mutant was constructed by the integration of pGIE007 (16) in the *acm2* mutant strain EP114 and was designated EP714.

Inactivation of Acm2 had a slight negative effect on growth during exponential phase, since the generation time of EP714 (150 min) is higher than that of EP007 (137 min) (Fig. 2A). Although the maximal OD_{600} at the entry of the stationary phase is similarly low in both mutant strains compared to that of the wild type, the decrease in OD_{600} observed during the stationary phase of the EP007 strain was suppressed by the inactivation of Acm2 in EP714 (Fig. 2A). In exponential phase (4 h), the same numbers of damaged cells were observed in the two strains (Fig. 2B), while during stationary phase (48 and 74 h), the number of EP714 injured cells was clearly reduced relative to that for EP007 (Fig. 2B). These data revealed that Acm2 is involved in the autolytic process that takes place during the stationary phase of growth of the *dlt* mutant.

Microscopy analysis of the double mutant revealed similar cell chains in both exponential and stationary phases as was observed for the single *acm2* mutant (Fig. 4C), indicating that Acm2 also performed the final separation of EP007 cells. Notably, no cell wall perforations were observed at any stage of growth in EP714 cells examined by SEM (Fig. 3F) or TEM (Fig. 3J), while dead V-shaped cells observed by epifluorescence microscopy were nearly absent in the EP714 cell population (data not shown). These observations demonstrate that Acm2 plays a key role in the formation of damage to the envelope of EP007 cells.

Concluding remarks. In most gram-positive species, four genes (*dltABCD*) are responsible for the incorporation of D-Ala into TAs. In *L. plantarum*, the *dlt* cluster is cotranscribed with the functionally distinct *pbpX2* gene, which is predicted to encode a D,D-carboxypeptidase involved in peptidoglycan biosynthesis. An in silico investigation of *dlt* loci from gram-positive bacterial genomes showed that the presence of *pbpX2* upstream of *dltA* is unique to *L. plantarum*. However, a *pbpX* homologue was found downstream of the *dlt* genes in *Lactibacillus acidophilus*, *Lactobacillus gasseri*, and *Lactobacillus johnsonii*, but experimental data with regard to cotranscription of these genes is unavailable to date. Interestingly, transcription of *pbpX* and that of of the *dlt* operon were recently shown to be under the control of the σ^X factor in *B. subtilis* (7). Besides the mutual

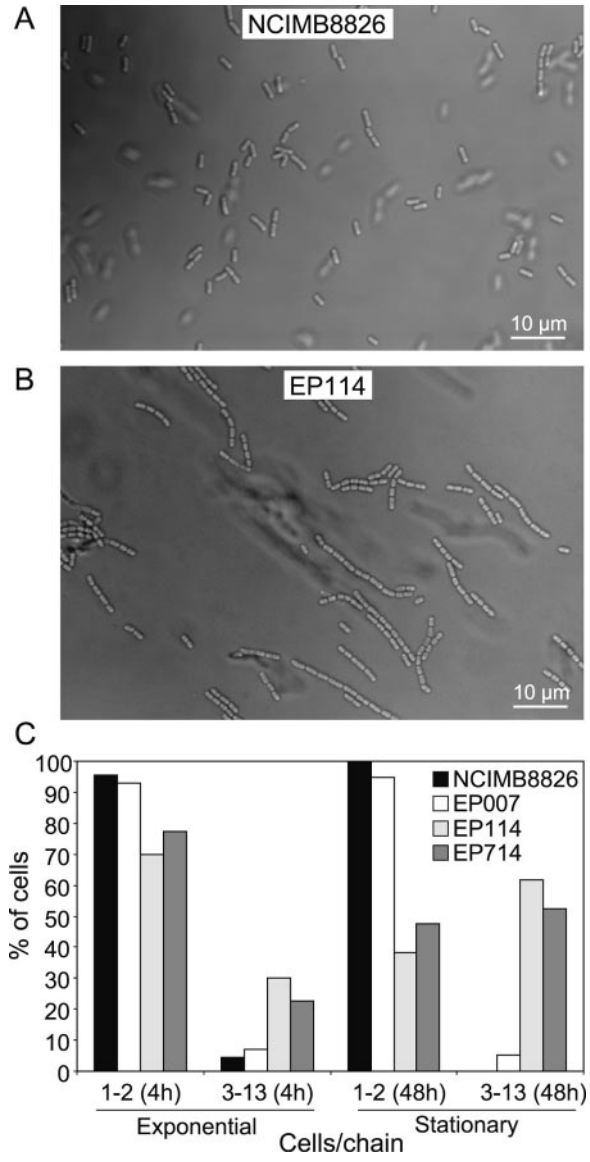

FIG. 4. Effect of *dlt*, *acm2*, and *dlt acm2* mutations on cell chain formation. Contrast phase micrographs of cells from NCIMB8826 (wild type; A) and EP114 (*acm2*; B) collected in stationary growth phase (growth conditions as described in Fig. 2 legend). (C) The number of cells per chain was measured for NCIMB8826, EP007, EP114, and EP714 in exponential (4 h) and stationary (48 h) growth phases. Percentage of cells corresponds to the number of individual cells over total cells that are present either isolated or in pairs (category 1-2) or included in chains of 3 to 13 cells (category 3-13). Measurements were performed on micrographs for a minimum of 300 cells per strain.

function in cell wall biosynthesis of *pbpX2* and *dlt*, the functional importance of their genetic linkage and/or cotranscription in *L plantarum* and other species remains to be established (7).

The inactivation of *dlt* in *L. plantarum* NCIMB8826 resulted in a deficiency of D-alanylation of LTA. Unexpectedly, this lack of D-Ala on LTA was partially replaced by glucose substitution, which was undetectable in wild-type LTA. The only similar observation reported in the literature was a doubling of the level of *N*-acetylglucosamine TA substituents in *dlt* mutants of *B. subtilis* (27). Moreover, the majority of LTA extracted from the *dlt* mutant of *L. plantarum* were threefold longer than LTA of the wild-type strain. Finally, the longest LTA were the least D-alanylated, suggesting a link between the level of D-alanylation and the elongation process, which might be correlated with the perturbation of the ionic environment of the LTA biosynthesis machinery. To the best of our knowledge, a similar alteration of the LTA length in other *dlt* mutants has never been reported before.

The major physiological changes displayed by the *dlt* mutant of *L plantarum* were a slower exponential growth rate accompanied by cell elongation and lysis during the exponential and stationary phases. These results show that the D-alanylation defect in *L plantarum* results in lysis in stationary phase and confirm previous observations with some other gram-positive bacteria, like *B. subtilis* (33) and *L. lactis* (32). However, in *L. plantarum*, in contrast to these bacteria, the lytic process had already started during exponential growth. Perforations of the cell envelope in the *dlt* mutant appeared in 20% of dividing cells (red V-shaped cells) in exponential phase and became gradually more numerous at the end of the exponential growth phase and during the stationary phase. These "holes" in the envelope are localized in the septal region, which suggests that the defect is linked to the cell separation process and the formation of the septum. By comparison, cell perforations were not observed during the exponential phase of the *dlt* mutant of *L. lactis* (data not shown). In addition, we showed that the predicted autolysin Acm2, necessary for the final separation of wild-type cells, was responsible for these cell perforations observed by electron microscopy in the *dlt* mutant of *L. plantarum*. Moreover, Acm2 involvement in lysis of the *dlt* mutant during the stationary phase could be demonstrated. Nevertheless, inactivation of Acm2 suppressed neither the slower growth, nor the presence of 20% of dead cells (propidium iodide labeled) during exponential phase, nor the detection of low numbers of dead cells in the stationary phase. In contrast, the growth defect and enhanced autolysis in stationary growth phase were completely suppressed by AcmA inactivation in the *L. lactis dltD* mutant (32). Although many proteins involved in the cell division and separation processes could be affected by the absence of D-alanylation, other autolysins predicted to be encoded in the *L. plantarum* genome (lp_2162, lp_3093, and lp_3421) (21) may be involved in this phenotype.

The characterization of the *L. plantarum dlt* mutant allowed us to evaluate the specific contribution of D-alanyl esters of TAs compared to the complete absence of D-Ala in both peptidoglycan and TAs, as has previously been described for the *L. plantarum alr* mutant (26). In this mutant, similar perforated cells were observed under D-alanine starvation, suggesting that the origin of these perforations was the lack of D-alanyl esters on TAs and depended on Acm2 activity. In contrast to the *alr* mutant, the *dlt* mutant does not show a thinning of the cell envelope, suggesting that this alteration is due to the absence of D-Ala in the peptidoglycan precursors, leading to a defect in peptidoglycan assembly. The recent construction of an *L. plantarum* cell wall mutant strictly deficient in the incorporation of D-Ala in peptidoglycan precursors confirms these observations. This mutant, unable to synthesize the D-Ala-D-Lac depsipeptide under D-lactate deprivation (15), shows a thinning of the

cell envelope but does not display cell wall perforations (P. S. Cocconcelli, P. Goffin, and P. Hols, unpublished).

Future work will aim at investigating the functional role of the two new genes discovered in the *dlt* operon, as well as the topological distribution of Acm2 and TA subtituents into the cell envelope of *L. plantarum*.

This research was carried out with financial support from the Commission of the European Communities, specific RTD project DEPRO HEALTH (QLK1-2000-00146). It does not necessarily reflect its views and in no way anticipates the commission's future policy in this area.

We thank R. Leer for providing PCR products of the *dlt* operon of *L. plantarum* at the start of this work. We thank R. R. Giorno for her help in the initial characterization of the *dlt* mutant. We warmly thank J. Delcour, P. Rouxhet, and F. C. Neuhaus for fruitful discussions and scientific advice. We thank D. Prozzi for critically reading the manuscript. E.P. holds a doctoral fellowship from FRIA. P.H. is Research Associate at FNRS.

REFERENCES

1. **Abachin, E., C. Poyart, E. Pellegrini, E. Milohanic, F. Fiedler, P. Berche, and P. Trieu-Cuot.** 2002. Formation of D-alanyl-lipoteichoic acid is required for adhesion and virulence of *Listeria monocytogenes*. Mol. Microbiol. **43:**1–14.
2. **Archibald, A. R., and J. Baddiley.** 1966. The teichoic acids. Adv. Carbohydr. Chem. Biochem. **21:**323–375.
3. **Boyd, D. A., D. G. Cvitkovitch, A. S. Bleiweis, M. Y. Kiriukhin, D. V. Debabov, F. C. Neuhaus, and I. R. Hamilton.** 2000. Defects in D-alanyl-lipoteichoic acid synthesis in *Streptococcus mutans* results in acid sensitivity. J. Bacteriol. **182:**6055–6065.
4. **Buist, G., H. Karsens, A. Nauta, D. van Sinderen, G. Venema, and J. Kok.** 1997. Autolysis of *Lactococcus lactis* caused by induced overproduction of its major autolysin, AcmA. Appl. Environ. Microbiol. **63:**2722–2728.
5. **Buist, G., J. Kok, K. J. Leenhouts, M. Dabrowska, G. Venema, and A. J. Haandrikman.** 1995. Molecular cloning and nucleotide sequence of the gene encoding the major peptidoglycan hydrolase of *Lactococcus lactis*, a muramidase needed for cell separation. J. Bacteriol. **177:**1554–1563.
6. **Bunthof, C. J., S. van Schalkwijk, W. Meijer, T. Abee, and J. Hugenholtz.** 2001. Fluorescent method for monitoring cheese starter permeabilization and lysis. Appl. Environ. Microbiol. **67:**4264–4271.
7. **Cao, M., and J. D. Helmann.** 2004. The *Bacillus subtilis* extracytoplasmic-function σ^X factor regulates modification of the cell envelope and resistance to cationic antimicrobial peptides. J. Bacteriol. **186:**1136–1146.
8. **Chen, J. D., and D. A. Morrison.** 1988. Construction and properties of a new insertion vector, pJDC9, that is protected by transcriptional terminators and useful for cloning of DNA from *Streptococcus pneumoniae*. Gene **64:**155–164.
9. **Clemans, D. L., P. E. Kolenbrander, D. V. Debabov, Q. Zhang, R. D. Lunsford, H. Sakone, C. J. Whittaker, M. P. Heaton, and F. C. Neuhaus.** 1999. Insertional inactivation of genes responsible for the D-alanylation of lipoteichoic acid in *Streptococcus gordonii* DL1 (Challis) affects intrageneric coaggregations. Infect. Immun. **67:**2464–2474.
10. **Debabov, D. V., M. P. Heaton, Q. Zhang, K. D. Stewart, R. H. Lambalot, and F. C. Neuhaus.** 1996. The D-alanyl carrier protein in *Lactobacillus casei*: cloning, sequencing, and expression of *dltC*. J. Bacteriol. **178:**3869–3876.
11. **Debabov, D. V., M. Y. Kiriukhin, and F. C. Neuhaus.** 2000. Biosynthesis of lipoteichoic acid in *Lactobacillus rhamnosus*: role of DltD in D-alanylation. J. Bacteriol. **182:**2855–2864.
12. **Delcour, J., T. Ferain, M. Deghorain, E. Palumbo, and P. Hols.** 1999. The biosynthesis and functionality of the cell-wall of lactic acid bacteria. Antonie Leeuwenhoek **76:**159–184.
13. **Derzelle, S., B. Hallet, K. P. Francis, T. Ferain, J. Delcour, and P. Hols.** 2000. Changes in c*spL*, *cspP*, and *cspC* mRNA abundance as a function of cold shock and growth phase in *Lactobacillus plantarum*. J. Bacteriol. **182:**5105–5113.
14. **Douglas, L. J., and M. J. Wolin.** 1971. Cell wall polymers and phage lysis of *Lactobacillus plantarum*. Biochemistry **10:**1551–1555.
15. **Goffin, P., M. Deghorain, J. L. Mainardi, I. Tytgat, M. C. Champomier-Verges, M. Kleerebezem, and P. Hols.** 2005. Lactate racemization as a rescue pathway for supplying D-lactate to the cell wall biosynthesis machinery in *Lactobacillus plantarum*. J. Bacteriol. **187:**6750–6761.
16. **Grangette, C., S. Nutten, E. Palumbo, S. Morath, C. Hermann, J. Dewulf, B. Pot, T. Hartung, P. Hols, and A. Mercenier.** 2005. Enhanced antiinflammatory capacity of a *Lactobacillus plantarum* mutant synthesizing modified teichoic acids. Proc. Natl. Acad. Sci. USA **102:**10321–10326.
17. **Hancock, I. C.** 2001. Teichoic acids of Gram-positive bacteria, p. 79–92. *In* M. Sussman (ed.), Molecular medical microbiology. Academic Press, San Diego, Calif.
18. **Heaton, M. P., and F. C. Neuhaus.** 1992. Biosynthesis of D-alanyl-lipoteichoic acid: cloning, nucleotide sequence, and expression of the *Lactobacillus casei* gene for the D-alanine-activating enzyme. J. Bacteriol. **174:**4707–4717.
19. **Heaton, M. P., and F. C. Neuhaus.** 1994. Role of the D-alanyl carrier protein in the biosynthesis of D-alanyl-lipoteichoic acid. J. Bacteriol. **176:**681–690.
20. **Hols, P., C. Defrenne, T. Ferain, S. Derzelle, B. Delplace, and J. Delcour.** 1997. The alanine racemase gene is essential for growth of *Lactobacillus plantarum*. J. Bacteriol. **179:**3804–3807.
21. **Kleerebezem, M., J. Boekhorst, R. van Kranenburg, D. Molenaar, O. P. Kuipers, R. Leer, R. Tarchini, S. A. Peters, H. M. Sandbrink, M. W. Fiers, W. Stiekema, R. M. Lankhorst, P. A. Bron, S. M. Hoffer, M. N. Groot, R. Kerkhoven, M. de Vries, B. Ursing, W. M. de Vos, and R. J. Siezen.** 2003. Complete genome sequence of *Lactobacillus plantarum* WCFS1. Proc. Natl. Acad. Sci. USA **100:**1990–1995.
22. **Kojima, N., Y. Araki, and E. Ito.** 1985. Structural studies on the linkage unit of ribitol teichoic acid of *Lactobacillus plantarum*. Eur. J. Biochem. **148:**29–34.
23. **Nakao, A., S. Imai, and T. Takano.** 2000. Transposon-mediated insertional mutagenesis of the D-alanyl-lipoteichoic acid (*dlt*) operon raises methicillin resistance in *Staphylococcus aureus*. Res. Microbiol. **151:**823–829.
24. **Neuhaus, F. C., and J. Baddiley.** 2003. A continuum of anionic charge: structures and functions of D-alanyl-teichoic acids in gram-positive bacteria. Microbiol. Mol. Biol. Rev. **67:**686–723.
25. **Neuhaus, F. C., M. P. Heaton, D. V. Debabov, and Q. Zhang.** 1996. The *dlt* operon in the biosynthesis of D-alanyl-lipoteichoic acid in *Lactobacillus casei*. Microb. Drug Resist. **2:**77–84.
26. **Palumbo, E., C. F. Favier, M. Deghorain, P. S. Cocconcelli, C. Grangette, A. Mercenier, E. E. Vaughan, and P. Hols.** 2004. Knockout of the alanine racemase gene in *Lactobacillus plantarum* results in septation defects and cell wall perforation. FEMS Microbiol. Lett. **233:**131–138.
27. **Perego, M., P. Glaser, A. Minutello, M. A. Strauch, K. Leopold, and W. Fischer.** 1995. Incorporation of D-alanine into lipoteichoic acid and wall teichoic acid in *Bacillus subtilis*. Identification of genes and regulation. J. Biol. Chem. **270:**15598–15606.
28. **Peschel, A., M. Otto, R. W. Jack, H. Kalbacher, G. Jung, and F. Götz.** 1999. Inactivation of the *dlt* operon in *Staphylococcus aureus* confers sensitivity to defensins, protegrins, and other antimicrobial peptides. J. Biol. Chem. **274:**8405–8410.
29. **Peschel, A., C. Vuong, M. Otto, and F. Götz.** 2000. The D-alanine residues of *Staphylococcus aureus* teichoic acids alter the susceptibility to vancomycin and the activity of autolytic enzymes. Antimicrob. Agents Chemother. **44:**2845–2847.
30. **Poyart, C., M. C. Lamy, C. Boumaila, F. Fiedler, and P. Trieu-Cuot.** 2001. Regulation of D-alanyl-lipoteichoic acid biosynthesis in *Streptococcus agalactiae* involves a novel two-component regulatory system. J. Bacteriol. **183:**6324–6334.
31. **Steen, A., G. Buist, K. J. Leenhouts, M. El Khattabi, F. Grijpstra, A. L. Zomer, G. Venema, O. P. Kuipers, and J. Kok.** 2003. Cell wall attachment of a widely distributed peptidoglycan binding domain is hindered by cell wall constituents. J. Biol. Chem. **278:**23874–23881.
32. **Steen, A., E. Palumbo, M. Deghorain, P. S. Cocconcelli, J. Delcour, O. P. Kuipers, J. Kok, G. Buist, and P. Hols.** 2005. Autolysis of *Lactococcus lactis* is increased upon D-alanine depletion of peptidoglycan and lipoteichoic acids. J. Bacteriol. **187:**114–124.
33. **Wecke, J., K. Madela, and W. Fischer.** 1997. The absence of D-alanine from lipoteichoic acid and wall teichoic acid alters surface charge, enhances autolysis and increases susceptibility to methicillin in *Bacillus subtilis*. Microbiology **143:**2953–2960.